Available online at www.sciencedirect.com
ScienceDirect
International Journal of Heat and Mass Transfer 51 (2008) 3164–3178
International Journal of HEAT and MASS TRANSFER
www.elsevier.com/locate/ijhmt

Development of optical digital interferometry technique for measurement of thermodiffusion coefficients

A. Mialdun, V.M. Shevtsova *

MRC, CP-165/62, Université Libre de Bruxelles, 50, av. F.D. Roosevelt, B-1050 Brussels, Belgium

Received 15 January 2007; received in revised form 16 August 2007
Available online 23 October 2007

Abstract

The paper presents the development of an experimental technique based on optical digital interferometry for measuring thermodiffusion (Soret) coefficients. The experiments are performed in a cubic cell containing an aqueous solution and being heated from above. This is the first report on the method that allows to record the temperature and concentration fields in the entire cell rather than just between two points. Such information is not only available at the steady state, but within the whole diffusion process. The time-dependent evolution of the concentration field allows the measurement of molecular diffusion coefficient in addition to the Soret coefficients. The measurements of transport coefficients have been performed in water/ethanol mixture and water/isopropanol mixtures.
© 2007 Elsevier Ltd. All rights reserved.

Keywords: Diffusion; Soret; Cubic cell; Optical digital interferometry; Aqueous solution

1. Introduction

Molecular diffusion occurs when a concentration gradient exists in a mixture: the net mass flux tends to decrease the magnitude of this concentration gradient. The mass flux in mixtures, which is induced by a temperature gradient is called the Soret effect or thermodiffusion. Knowledge of transport properties in liquid mixtures is important for applications [1,2].

Transport coefficients in gases can be rather well estimated by kinetic theory but the situation is less favorable for liquid mixtures. Thermal diffusion in liquids is not so well understood even for binary mixtures [3–6]. One of the peculiarities of thermodiffusion in some aqueous solutions and organic mixtures is that the Soret coefficient may change sign depending on composition and temperature.

The numerical models based on different assumptions are not complete and they should be more extensively verified by experimental measurements. A variety of different experimental techniques is used for the measurements of Soret effect in liquids. Two recent reviews have summarized the current experimental approach [7,8]. Roughly the experimental methods can be divided into two classes: (1) methods that employ the presence of buoyant convection in the measurements; (2) methods in which buoyant convection plays deleterious role and efforts are done to minimize its effect.

The major part of the second group is the optical methods which rely on the variation of refractive index with composition. The main features of optical methods are non-intrusiveness and sensitivity. A significant advantage of these methods is the absence of mechanically driven parts in contact with liquid, so measurements do not disturb the experiment. The main disadvantage is that the media under investigation must be transparent. Recent advances in lasers and electronic cameras as well as increasing possibilities of computer-aided data processing have enabled considerable progress in the development of new optical measurement techniques along with a revival of traditional techniques.

* Corresponding author. Tel.: +32 2 650 30 24; fax: +32 2 650 31 26.
E-mail address: vshev@ulb.ac.be (V.M. Shevtsova).

0017-9310/$ - see front matter © 2007 Elsevier Ltd. All rights reserved.
doi:10.1016/j.ijheatmasstransfer.2007.08.020

Nomenclature

C	concentration, mass fraction of water
D	diffusion coefficient
d	wall thickness
$\mathbf{j}$	flux
L	cell size
n	refractive index
S_T	Soret coefficient, $\widetilde{S}_T = S_T C_0(1-C_0)$
T	temperature
T_{hot}, T_{cold}	temperatures of top ant bottom walls
$T_{\mathrm{mean}} = T_{\mathrm{cold}} + \Delta T/2$	mean temperature
t	time

Greek symbols

$\Delta T = (T_{\mathrm{hot}} - T_{\mathrm{cold}})$	applied temperature difference
$\Delta\varphi$	phase change
λ	wave length
κ	heat conductivity
ρ	density
τ_{th}	thermal time
τ_{D}	diffusion time
τ_{r}	relaxation time
χ	thermal diffusivity

One of the traditional techniques is a beam-deflection method, which was used, e.g. by Giglio and Vendramini [9] to study the buoyancy-driven instability occurring in a dilute polymer solution characterized by a negative value of the thermodiffusion ratio. Later on it was adopted by Kolodner et al. [10] for water/ethanol mixtures. The beam-deflection technique was improved by Zhang et al. [11] and applied to measurements of Soret coefficients in mixtures of toluene and *n*-hexane. In this technique the transparent optical (diffusion) cell is filled with the test liquid and heated from above in order to minimize free convection. The vertical temperature and concentration gradients are measured by the deflection of laser beam (due to the refractive index gradient) propagating through the liquid mixture parallel to horizontal walls kept at different temperatures.

Another optical method employs a transient holographic technique. It is based on thermal diffusion forced Rayleigh scattering and is actively used nowadays [12,13]. A grating created by the interference of two laser beams of equal intensity is written into a sample. A small amount of dye dissolved in the sample converts the intensity grating into a temperature grating, which in turn causes a concentration grating by the effect of thermal diffusion. Both gratings contribute to a combined refractive index grating, which is read by a third laser of different wavelength. Thus, the light is used to create a temperature gradient inside small zone of a liquid instead of differentially heated rigid walls.

It should be mentioned that all these methods measure only the concentration difference between a hot and a cold plates/zones or between central line and some point. We present a method which allows measuring not only ΔC between the hot and cold plates, but also the concentration and temperature distributions along the diffusion path. Knowledge of the spatial temperature and concentration fields enables to examine the appearance of convective flows, to localize them and to study influence of these flows on the measured values of the Soret and diffusion coefficients. All methods developed to measure thermodiffusion coefficients are affected by convection on one or another scale and to the best of our knowledge such a study of the role of convection has not been undertaken.

The objective of this paper is to present details of the development of a new technique based on optical digital interferometry and to utilize it to investigation of the thermal diffusion process in water/ethanol and water/isopropanol mixtures.

2. Experimental method

2.1. Principle of the experimental method

A new experimental set-up was designed to study heat and mass transfer in liquids with Soret effect. The suggested instrument consists of two principal parts: the optical cell (in some way similar to that used earlier [11,14]) and an interferometric system in combination with equipment for digital recording and processing the phase information. This technique allows performing and reproducing experiments without disturbing the media. The reliability of the experiments can be improved in an important way by using statistical means [16,17]. It gives possibility to adopt this technique for some other purposes, for example to study hydrodynamic fluctuations [15].

The experiments were performed in a transparent cubic cell filled initially by a homogenous mixture. The thermal gradient is imposed by heating and cooling the top and bottom walls of the cell, respectively. The spatial temperature variation induces mass transfer through the Soret effect. An enlarged collimated laser beam traverses the entire cell perpendicular to the temperature gradient. Both temperature and composition variations contribute to the spatial distribution of the refractive index that modulates the wave-front of the emerging optical beam. Using an interferometric technique the final wave-front shape is accurately determined by comparison with undisturbed shape. The optical interferometer coupled with a digital recording and processing is used for very accurate determination of a phase shift. Each interferogram is reconstructed by performing a 2D fast Fourier transform (FFT) of the fringe image, filtering a selected band of the spectrum,

performing an inverse 2D FFT of the filtered result and phase unwrapping. Knowledge of phase shifts gives information about the local gradients of refractive index. Then the gradients of composition inside of the fluid are calculated from refractive index gradients and local temperature both for steady state and dynamic regimes. Thus optical digital interferometry enabled measurements of ΔC between two arbitrary points.

2.2. Experimental set-up

The set-up was developed using the concept of a Mach–Zehnder interferometer as it is shown in Fig. 1. The light beam of constant frequency He–Ne laser (wavelength $\lambda = 632.8$ nm) is expanded by the spatial filter (L) and then passes through the beam splitter (BS) where it is splitted into two beams of equal intensity. One of them goes through the experimental cell (C). After passing mirrors (M) the object and reference beams interfere with each other at the second beam splitter (BS). Finally interference fringes are captured by the CCD camera (1280 × 1024) pixels sensor; image scale is approximately 50 pixels/mm. It is possible to modify the distance between fringes by changing the incident angle of the object and the reference beams by adjusting the inclination angle of one the mirrors M. The efforts were aimed to decrease this distance to 3–4 pixels to obtain the larger number of fringes in the field of view.

An optical cubic cell of internal size $L = 10$ mm is made of quartz *Suprasil* by the Hellma company. From the first look the distance $L = 10$ mm between differently heated walls is too large for usual diffusion experiments. The present configuration enables the study of the temporal and spatial behavior of the temperature and the concentration

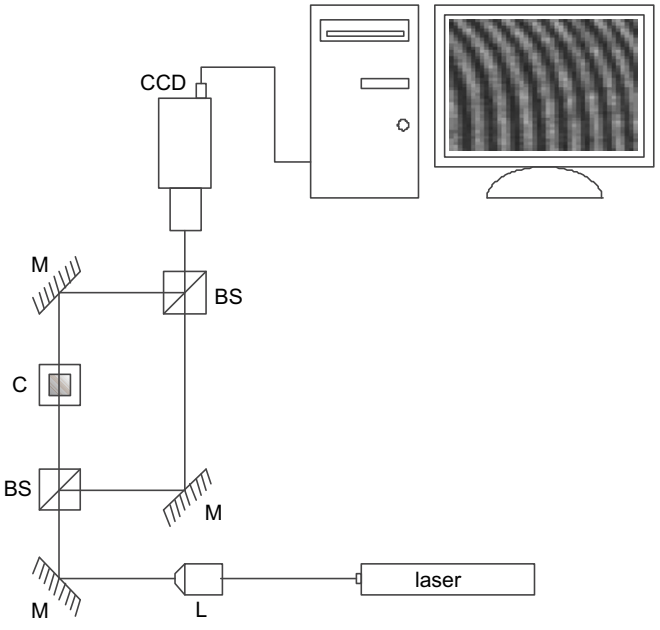

Fig. 1. Scheme of the set-up.

fields. On the basis of this knowledge we may adjust optical part in a best way and improve the thermal design, see discussion in Section 4. Also this cell size is helpful for identification and examination of deleterious convection, see Section 6.1. Having solved all problems and knowing the weak and strong points of this technique, the cell height can be diminished at least twice without loosing the quality of experimental results.

The top and bottom of the cell are kept at constant temperatures (T_{hot} and T_{cold}, respectively) by Peltier modules (3 cm × 3 cm) driven by Wavelength Electronics PID temperature controllers. So, the Peltier modules and correspondingly, copper plates, are essentially larger than the cell. Our observation showed that the stability of temperature maintained by the controllers is 0.02–0.05 K for typical experimental time (several days), although manufacture company gives value by one order of magnitude smaller. External sides of Peltier modules are kept as close as possible to the room temperature by using heat sinks with small fans. The rotation speed of the fans was optimized with respect to the thermal resistance and the noise introduced into the optical measurements by the generated airflows. A filling system for the cell is developed which allows accurate liquid injection and pressure release when the liquid is heated up.

To reduce the possibility of convection caused by temperature gradients in horizontal direction the leveling of the cell has to be checked. The levels of top and bottom copper plates were checked by cathetometer WILD Heerbrugg (Switzerland), model KM 345. With this procedure the plates were leveled to a maximal inclination of 2.5 ± 0.2 mrad.

The entire set-up was mounted on the optical table Melles Griot with pneumatic damping control to isolate it from external mechanical vibrations. To assess the short term ($t \leqslant 5$ min) and long-term ($t = 120$ h) stability of the interferometer few tests were performed. The set-points of thermal regulators (for both plates of the cell as well as for the box regulator) were settled to the same temperature 299 K. The phase recordings both in the cell and in the air, close to the cell, were taken every second during 5 min and every 30 min for 120 h. Our method of extracting the temperature and concentration from the phase shift needs only the relative value of the phase. To estimate the relative value, phase differences between the first record and all subsequent ones were calculated, $\Delta\phi(x,\ z,\ t_i) = \phi(x,\ z,\ t_i) - \phi(x,\ z,\ t_0)$. At the next step spatial mean value over entire field of view was defined

$$\Delta\phi_{\mathrm{mean}}(t_1) = \frac{1}{N}\sum_{i=1,N}\Delta\phi(x_i, z_i, t_1)$$

Then the deviations from mean value were calculated $\delta\phi(x,\ z,\ t_1) = \Delta\phi(x,\ z,\ t_1) - \Delta\phi_{\mathrm{mean}}(t_1)$, which were used to determine the change of refractive index. During the interferometer stability tests the standard Gaussian deviation of the differences over all pixels was evaluated. For short term

the standard deviation of the phase is 0.16 rad, while for long term it is 0.38 rad, $\Delta T = 0$. Corresponding results in air displayed much smaller values: 0.02 rad and 0.05 rad. It results in excellent stability of the phase at this particular region. The phase shift induced by thermodiffusion process is at least three order of magnitude larger. We consider that for proving the long-term mechanical stability it is a satisfactory test. Taking into account the good quality of the laser, the interferometer stability is mainly related to mechanical stability. Besides the phase change was measured in the middle of the experimental cell during ≈30–50 h (at the end of experiment) when the steady state in the central part of the cell was achieved. The measurements showed perfect stability of the phase at this particular region.

Nevertheless, we decided to perform an extra test to remove any doubts. This test was performed in air, while the experiment was running in the cell ($\Delta T = 10$ K). The maximal standard deviation of the phase for the long term test was about 0.5 rad. The measurements were done at the same point as for $\Delta T = 0$. Note that the magnitudes of the measured phase differences of physical quantities are about 350 rad, see Fig. 3.

2.3. Experimental procedure

A typical experiment was carried out as follows. The cell was filled with a binary mixture and inserted into the experimental structure. Then the Peltier modules established the temperature of the top and bottom plates equal to the mean temperature of the planned experiment. A waiting period of at least 2 h was allowed in order to reach a steady state. Two thermistors, inserted inside the cold and hot plates, were used for temperature control. A third thermistor and one thermocouple were utilized for the control of air temperature. The thermistors were regularly calibrated using a certified platinum resistance thermometer PT100. During this procedure all thermistors were placed simultaneously in the calibration bath (Thermo Electric, CAL-31502, USA) the temperature of which was varied in the working range with the step 2 K. The temperature difference between plates was maintained with accuracy not less than 0.01 K.

Before setting ΔT to a designated value a first image was acquired at $T = T_{\text{mean}}$ and used for the reconstruction of a reference phase. This reference interference pattern is obtained by using both the reference and the object beams. This interferogram includes all the phase shifts caused purely by the optical and mechanical elements of the system. This knowledge is important for processing all subsequent interference images. Immediately after applying the temperature gradient interferogram acquisition was quite frequent (1/min during 20 min) to record the developing thermal field. The time step between image acquisitions was gradually enlarged up to half an hour for tracking the much slower thermodiffusion separation. To approach to the stationary state a typical experimental time was a few days.

3. Refractive index

After fringe analysis one gets a spatial distribution of the total phase shift in the object beam caused by the optical properties of the liquid. Assume that the initial refractive index of the homogeneous mixture is $n_0(T_0, C_0)$, after a short period of time the refractive index changes to $n(x, z, t)$ at the point (x, z) (temperature and concentration variation). The change of the refractive index Δn may be obtained from the unwrapped phase change $\Delta\varphi$ using the expression:

$$\Delta n = n(x,z) - n_0 = \frac{\lambda}{2\pi L}\Delta\varphi \tag{1}$$

where λ is the wavelength and L is the thickness of the liquid in the direction of the optical pathway. For the given wavelength, the variation of the refractive index includes temperature and concentration contributions

$$\Delta n(x,z,t) = \left(\frac{\partial n}{\partial T}\right)_{T_0,C_0}\Delta T(x,z,t) + \left(\frac{\partial n}{\partial C}\right)_{T_0,C_0}\Delta C(x,z,t) \tag{2}$$

where $\Delta T(x, z, t)$ and $\Delta C(x, z, t)$ are temperature and concentration variations at point (x, z). For correct measurements we have first to find the optical contribution of the cell material because the laser beam passes through both the container and the solution. The total phase shift variation at the observed point can be written as

$$\Delta\varphi(x,z,t) = \Delta\varphi_{\text{liquid}}(x,z,t) + 2\Delta\varphi_{\text{cell}}(z,t)$$

In the field of view there are some regions where light beam goes only through glass (side walls). Having in hands directly measured $\Delta\varphi_{\text{cell}}$ the change of the refractive index of glass Δn_{cell} due to applied temperature difference ΔT can be easily evaluated

$$\Delta n_{\text{cell}} = \frac{\lambda}{2\pi(L+2d)}\Delta\varphi_{\text{cell}}$$

where d is the thickness of the cell walls. This experimental value Δn_{cell} can be cross-checked by Eq. (2) using the data for $(\partial n/\partial T)$ from the literature while $\Delta C = 0$. Note, that $(\partial n/\partial T)$ coefficient for glass is one order of magnitude less than for liquid and may be presumed constant in the studied temperature range.

Refractive index variations $(\partial n/\partial C)$ and $(\partial n/\partial T)$ as a function of mixture composition are shown in Fig. 2 at the temperature $T \approx 293$ K. At first step the data in Fig. 2 were taken from different sources in literature (see e.g. [19,18]) and the points of particular interest were verified by Abbe refractometer operating at wavelength $\lambda_D = 589.3$ nm. The open circles correspond to our laboratory measurements. They are in agreement with generalized literature data.

Fig. 2a shows that the derivative $(\partial n/\partial C)$ changes sign when the mass fraction of water is about 0.08. Since the magnitude of $\partial n/\partial C$ in the vicinity of this point is very

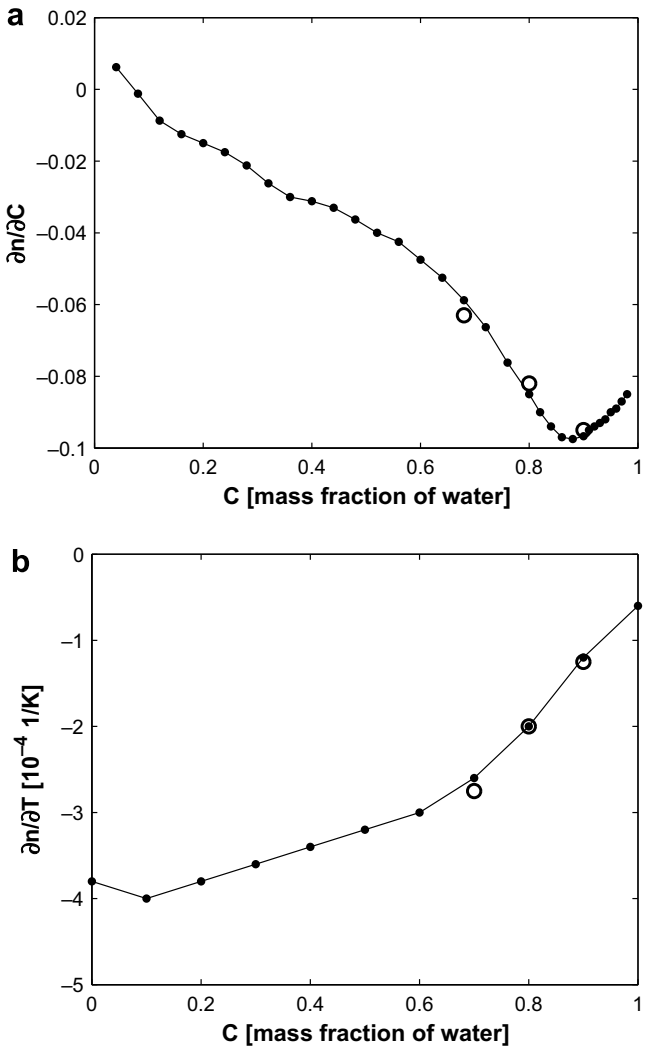

Fig. 2. Variations of (a) $(\partial n/\partial C)$ and (b) $(\partial n/\partial T)$ as a function of mass fraction of water given by [19,18]. The open circles correspond to our laboratory measurements.

small, measurements based on optical techniques will be inaccurate. The temperature dependence $(\partial n/\partial T)$ shown by Fig. 2b is growing function of water content being negative on whole range and the order of magnitude is about $\sim 10^{-4}\,\mathrm{K}^{-1}$. The refractive index variations $(\partial n/\partial T)$ and $(\partial n/\partial C)$ are assumed constant for each particular mixture in the narrow $T-C$ region under investigation ($\Delta T < 10$ K, $\Delta C < 0.02$). To recalculate the data in Fig. 2 to the laser beam wavelength, i.e. $\lambda = 632.8$ nm, one should use Cauchy dispersion relations

$$n(\lambda) = n_\infty + \frac{A}{\lambda^2}$$

where two parameters (n_∞ and A) have to be determined, see for example [20]. Favourably, the data in literature state that, at considered temperature range, the difference in refractive indices of the pure fluids (i.e. water and isopropanol) changes by only 0.2% on going from 589.3 nm to 632.8 nm. At first stage it allows us to consider with a reasonable accuracy that $(\partial n/\partial C)$ and $(\partial n/\partial T)$ are independent of wavelength.

Because two very different time scales are involved in the process, Eq. (2) can be decomposed. Starting with an isothermal homogeneous binary mixture and applying a temperature gradient a concentration profile will set-up due to Soret effect. The steady temperature distribution will be established after a characteristic time $\tau_{\mathrm{th}} = L^2/\chi \approx 770$ s which depends on the size L of the experimental cell and on the thermal diffusivity χ of the binary mixture. Simultaneously mass separation occurs along the temperature gradient. However, mass transport is significantly slower than the thermal process; its characteristic time τ_{D} is usually two orders of magnitude larger than the thermal time τ_{th}; $\tau_{\mathrm{D}} = L^2/D \approx 115 \times 10^3$ s; here D is the diffusion coefficient. Thus the temperature dependent component of the refractive index will reach constant value relatively fast. The refractive index is calculated from the phase difference, see Eq. (1). The evolution of the phase difference with time is shown in Fig. 3 for water/isopropanol mixture with initial mass fraction of water $C = 0.5$. The main graph presents the progress on long time scale and insertion displays the process on short time scale. The latter one demonstrates that the phase shift achieves the horizontal plateau corresponding to the establishment of temperature gradient somewhat in 5 min. From the images recorded early in time (first 5–10 min) one can define $\Delta T(x, z, \tau_{\mathrm{th}}) = \Delta T_{\mathrm{ref}}(x, z)$

$$\Delta n(x,z,t) = \left(\frac{\partial n}{\partial T}\right)_{T_0,C_0} \Delta T_{\mathrm{ref}}(x,z,t)$$

and later in time the refractive index will change only due to the Soret induced variations of concentration field

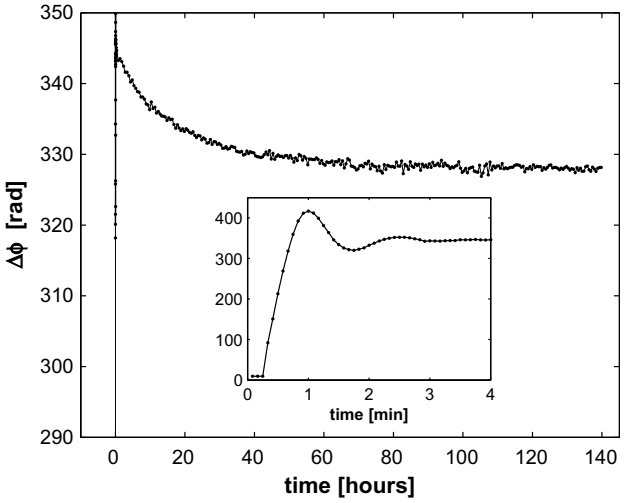

Fig. 3. Evolution of the phase difference $\Delta\phi = \phi_{\mathrm{bottom}} - \phi_{\mathrm{top}}$ with time during thermodiffusion experiment. Insertion demonstrates the phase change on short time scale when all changes are only due to the establishment of temperature gradient; water/isopropanol mixture with $C_0 = 0.5$.

$$\Delta n(x,z,t) = \left(\frac{\partial n}{\partial T}\right)_{T_0,C_0} \Delta T_{\mathrm{ref}}(x,z) + \left(\frac{\partial n}{\partial C}\right)_{T_0,C_0} \Delta C(x,z,t) \tag{3}$$

The main graph in Fig. 3 demonstrates slow variation of phase shift due concentration modulation within the mixture with initial water content $C_0 = 0.5$. The visible variation of the concentration lasts at least 60 h (about two diffusion time). At the end of the experiment, when the system is reverted to an isothermal case ΔT, the molecular diffusion will progressively reduce the previously established concentration gradient. Again, the steady temperature distribution will be rapidly established and we can verify once more the reference value $\Delta T_{\mathrm{ref}}(x, z)$.

4. Environmental conditions

The environmental conditions at which the experiments are carried out, drastically influence the quality of the results. Time evolution of concentration differences between top and bottom within the cell, $\Delta C(t)$, is shown in Fig. 4 for water/isopropanol system with different mass fraction of water: $C_0 = 0.5$, 0.6, and 0.7. Discrete symbols correspond to the numerous experimental points and the solid lines present the fitting curves according to Eq. (13) in Section 5. After carefully analyzing these time histories, i.e. $\Delta C = \Delta C(t)$, we found out that the experimental points perform periodic oscillations around the fitting curves. The time scale of the fluctuation periods indicated that they are related to daily temperature variations. For long duration experiments of several days it has no dramatic effect, but for short experiments it may significantly affect the values of the measured coefficients.

A detailed study was performed to understand the influence of the environmental conditions on the experimental results using a water/isopropanol mixture with initial mass fraction $C_0 = 0.5$. Three different types of environmental conditions were examined: (1) the experimental apparatus was in open air at room temperature; (2) the entire set-up was enclosed in a thermostabilized box of size [0.85 m × 0.50 m × 0.30 m] made of heat insulating material. The temperature inside the box was kept constant by additional heaters; (3) the entire set-up was enclosed in the same thermostabilized box but with additional shielding plates that would interrupt the gas flow inside box.

The results from these experiments as the function $\Delta C = \Delta C(t)$ are shown in Fig. 5a by open circles, filled dots and open squares, respectively. The number of experimental points is huge. Solid lines show the fitting curves. To make the presentation of the results more clear the initial part of the plot ($t < 20$ h) is cut off. Unlike other similar plot for time evolution of ΔC, shown in Fig. 4, the

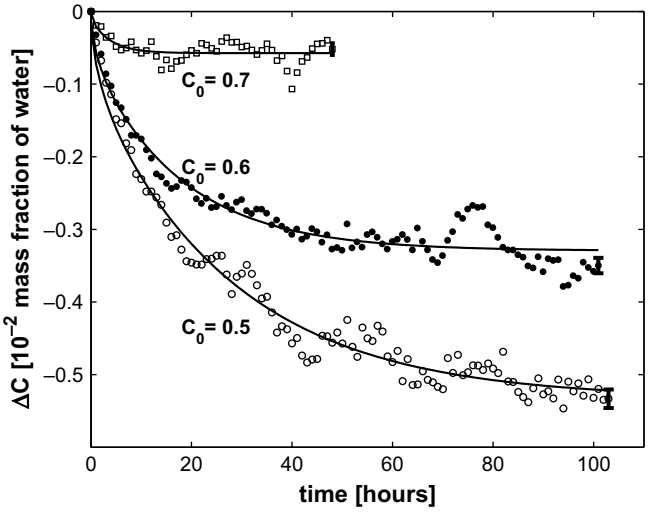

Fig. 4. Time evolution of concentration separation $\Delta C(t)$ for different compositions: $C_0 = 0.5$, 0.6, and 0.7 (water/isopropanol system).

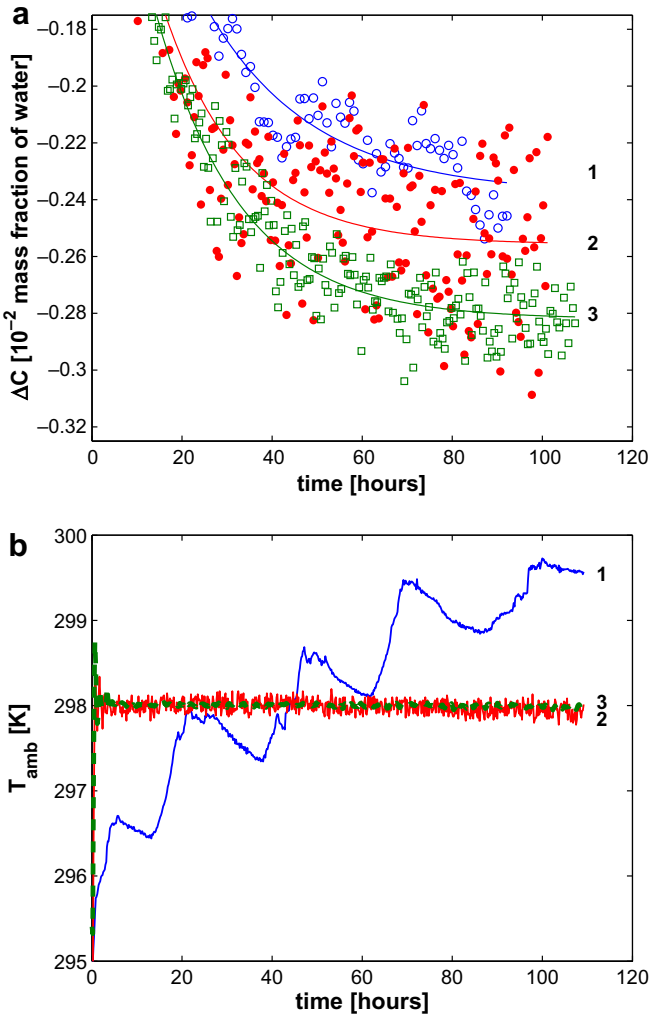

Fig. 5. The role of environmental conditions. Time evolution of (a) component separation and (b) ambient temperature during $t = 110$ h $\approx 35\tau_r \approx 4\tau_D$. Solid curves on the left graph correspond to interpolations of measured values. Curve 1 and open circles – the cell is in ambient conditions, curve 2 and filled circles – the cell is placed into a thermostabilized box, curve 3 and open squares – the cell is in the thermostabilized box with interruption of air convection.

information for this plot was taken from the central part of the cell where convection is absent (as explained in Section 6.1). The variations of the temperature with time in the air near the cell are shown in Fig. 5b for the same environmental conditions as in Fig. 5a by curves 1–3.

In the experiments where the cell is surrounded by open air the component separation $\Delta C(t)$ as well as the temperature of the air (open circles and curves 1 in Fig. 5) perform oscillations with a period of about 24 h. Such type of behavior was observed in the experiments with all the considered water/isopropanol mixtures. Note that the variations in room temperature during these experiments were about 1.5 K per day.

Thermostabilizing completely eliminated daily oscillations. The average temperature near the cell and optics is somewhat constant with small variation of ±0.1 K, see curve 2 in Fig. 5b. However, the time dependence, $T(t)$, displays high frequency oscillations with small amplitude. Unexpectably it caused the new problem of rising high frequency noise in the measured ΔC values. It results in the large disordered scattering of the experimental points that overlaps all the displayed results; in Fig. 5a there are some filled dots (red dots online) above curve 1 and below curve 3. This is due to intensive buoyant convection in the gas phase around the cell driven by the various heat sources in the closed volume that strongly perturb the interferometry. Thus for the optical methods the convection in surrounding gas is as dangerous as convection inside the cell.

In the third case study two large plates, interrupting the gas flow, were inserted in the box to eliminate convection in gas phase. The experimental points for this case are shown in Fig. 5a by open squares and the temperature variation with time is shown as curve 3 in Fig. 5b. The temperature in the air is kept constant. The scattering of the results is much smaller in this case and we consider the results obtained under these environmental conditions as reliable. Quantitative comparison of the results for different environmental conditions will be given in Section 6.4.

5. Theoretical approach

In the absence of motion the mass transport of species is driven by compositional and thermal gradients. The heat and mass diffusion fluxes can be written as

$$\mathbf{j_T} = -\kappa \nabla T \tag{4}$$

$$\mathbf{j_C} = -\rho(D\nabla C + D_T C(1-C)\nabla T) \tag{5}$$

Hereafter common approximation $C(1-C) \approx C_0(1-C_0)$ suitable in the case of small concentration variations will be used. Here κ is the heat conductivity (note that $\chi = \kappa/\rho c_p$); D and D_T are the diffusion and thermal diffusion coefficients, respectively. Heat and mass conservation require

$$\rho c_p \frac{\partial T}{\partial t} = -\nabla \mathbf{j_T}$$

$$\frac{\partial C}{\partial t} = -\nabla \mathbf{j_C}$$

so, the governing equations for motionless fluid can be written as

$$\frac{\partial T}{\partial t} = \chi \nabla^2 T \tag{6}$$

$$\frac{\partial C}{\partial t} = D\nabla^2 C + D_T C(1-C)\nabla^2 T \tag{7}$$

Eqs. (6) and (7) have to be solved subject to the following boundary conditions: (a) no mass flux $\mathbf{j_C} \cdot \mathbf{n} = 0$ through the impermeable rigid walls (here $\mathbf{n}$ is the unit normal vector to a wall); (b) heating from the top while the bottom side is kept at lower constant temperature; and (c) thermally insulated lateral walls.

Here under the Cartesian coordinate system will be used, where z-axis is directed from the cold to the hot wall with the origin $z = 0$ on the cold side. The following assumptions are introduced:

- T, C are only functions of the vertical coordinate and time $T = T(z, t)$, $C = C(z, t)$;
- the temperature distribution sets up instantly, i.e. $\partial_t T = 0$, consequently, the temperature profile is linear across the cell, so $\partial T/\partial z = \Delta T/L$. Under these assumptions the mass flux is written as

$$\vec{j}_C = -\rho_0[D\nabla C + D_T C_0(1-C_0)\Delta T/L]$$

Then Eq. (7) becomes

$$\frac{\partial C}{\partial t} = D\frac{\partial^2 C}{\partial z^2} \tag{8}$$

Absence of mass flux $\mathbf{j_C} \cdot \mathbf{n} = 0$ through the rigid walls leads to

$$\frac{\partial C}{\partial z} + \widetilde{S}_T \Delta T/L = 0 \tag{9}$$

where $\widetilde{S}_T = S_T C_0(1-C_0)$ and S_T is the Soret coefficient. Eq. (8) can be solved by separation of variables

$$C(z,t) = (A_n \cos \alpha_n z + B_n \sin \alpha_n z)\mathrm{e}^{-\alpha_n^2 Dt}$$

The solution (9) satisfying boundary conditions can be written in the form

$$C(z,t) = C_{st}(z) + \sum_{n=1}^{\infty} A_n \cos\left(\frac{n\pi z}{L}\right) \exp\left(-\frac{n^2\pi^2}{L^2} Dt\right) \tag{10}$$

where $C_{st}(z)$ is the steady-state linear concentration profile across the cell with slope defined by the boundary condition. On this profile the concentration in middle of the cell is equal to the initial value $C(L/2, t) = C_0$, and is given by

$$C_{st}(z) = C(t \to \infty, z) = C_0 + \widetilde{S}_T \frac{\Delta T}{L}(L/2 - z) \tag{11}$$

The constants A_n are determined from the initial conditions $C(z, t = 0) = C_0$:

$$A_n = -\frac{2[1-(-1)^n]}{n^2\pi^2}\widetilde{S}_T \Delta T$$

$A_n \neq 0$ only for odd n so that

$$A_n = -\frac{4}{n^2\pi^2}\widetilde{S}_T\Delta T$$

The solution of Eq. (10) can be written as

$$C(z,t) = C_0 + \widetilde{S}_T\Delta T\left[\frac{1}{2} - \frac{z}{L} - \frac{4}{\pi^2}\sum_{n,\mathrm{odd}}^{\infty}\frac{1}{n^2}\cos\left(\frac{n\pi z}{L}\right)\exp\left(-n^2\frac{t}{\tau_r}\right)\right] \quad (12)$$

Here $\tau_r = L^2/\pi^2 D$ is the relaxation time. In order to process the experimental results we first followed an often used procedure. The change of the concentration difference between top and bottom within the cell $\Delta C(t) = C(L, t) - C(t)$ with time was measured via the refractive index. On the other hand $\Delta C(t)$ can be found from Eq. (10)

$$\Delta C(t) = \widetilde{S}_T\Delta T\left[1 - \frac{8}{\pi^2}\sum_{n,\mathrm{odd}}\frac{1}{n^2}\exp\left(-n^2\frac{t}{\tau_r}\right)\right]. \quad (13)$$

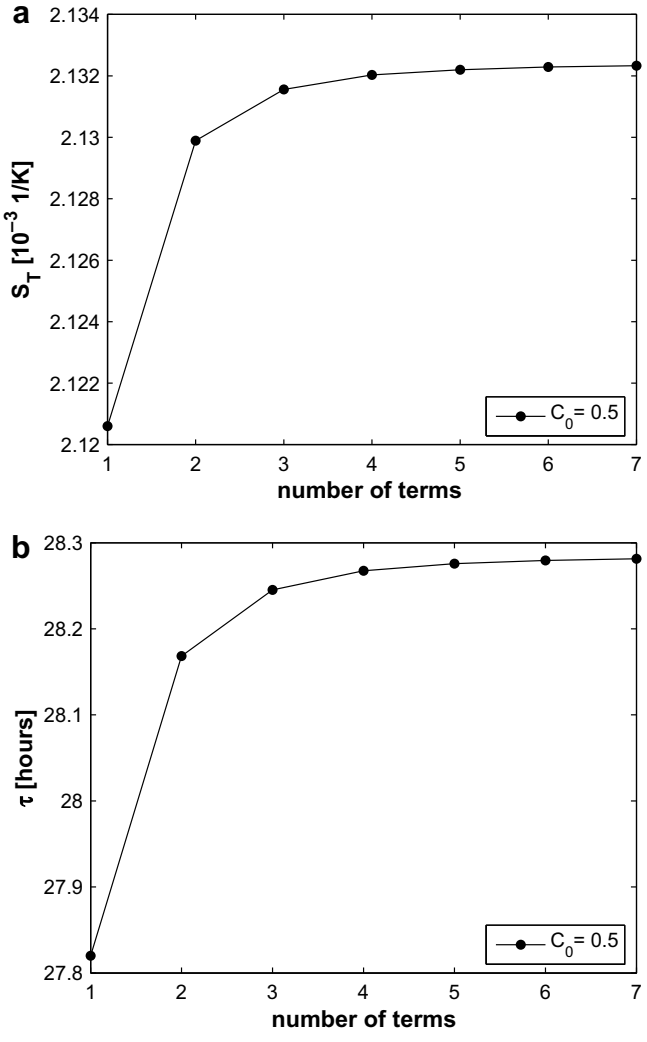

Fig. 6. The dependence of (a) S_T and (b) τ upon the number of retained terms N in Eq. (13).

In Eq. (13) there are two unknown parameters: the Soret coefficient S_T and the relaxation time τ_r. We collect experimental points $\Delta C(t)$ from the beginning to several characteristic times and the two parameters S_T and τ_r are fine-tuned until Eq. (13) fits the experimental results best. For this purpose a curve fitting procedure of the MatLab software is used. In addition to the determination of the Soret coefficient, the diffusion coefficient is derived from the value of the relaxation time τ_r. The accuracy of the results depends on the number of terms N retained in Eq. (13). The dependence of S_T and τ_r on N in Eq. (13) is shown in Fig. 6 for the initial composition of mixture $C_0 = 0.5$ after long duration experiment, $t = 110$ h. It is seen that four or five terms give reasonably good accuracy. Five terms will be used throughout this study.

6. Results and discussion

The proposed technique was initially developed for future experiments in microgravity where buoyant convection is negligibly small. While designing the set-up we realized that this method can be used in laboratory conditions with some precautions. Moreover, we found out that we are able to study appearance of parasitic convection, measure its velocity, identify the reasons and localize the convection-free region. The results presented below correspond to a possible minimal convection level on the ground. A set of experiments was done with water/ethanol and water/isopropanol mixtures belonging to the concentration region with positive Soret coefficient. No hydrodynamic instabilities are expected for these mixtures. The mean temperature in these experiments was kept at ~298 K and ΔT was about 10 K, although some experiments were repeated for $\Delta T \sim 5$ K.

6.1. Identification of convection

Optical digital interferometry enabled measurements of ΔC not only between the hot and cold plates, but also between two arbitrary points. Thus the transient concentration and temperature distributions can be restored along the whole diffusion path.

The concentration and temperature profiles for the initial composition $C_0 = 0.5$ in water–isopropanol mixture are shown in Fig. 7 at steady state, when $t = 110$ h $\approx 35\tau_r \approx 4\tau_D$. The solid lines correspond to the experimentally measured profiles and the dashed lines show linear extensions. To build these profiles the temperature and concentration in the region adjacent to the lateral walls were cut off for each vertical position z. The values of C and T at the remaining points of this horizontal line were averaged. For all examined mixtures (not only for composition shown in Fig. 7a) the temperature profile is almost linear; small deviations are observed only near the horizontal walls. The concentration profile is also linear in the central part of the cell. But moving away from the central part the deviations grow noticeably.

There are two apparent reasons that may perturb the concentration profile: undesirable convection due to horizontal temperature gradients and bubbles. The problem of bubble prevention was discussed in [21] and solution has been found. Despite the heating from above, convection in the cell occurs in the laboratory experiments for the working range of temperature difference. The stationary temperature field is shown in Fig. 8 at the beginning of the experiment, $t = 1200$ s. At that time the temperature field is already established $t > \tau_{th} = 770$ s, but the diffusion process did not begin, $t \ll \tau_D = 1.15 \times 10^5$ s. Fig. 8 demonstrates that the temperature field is basically linear and relatively small deviations arise approaching to the corners. These small local horizontal gradients cause buoyant convection. For all examined aqueous solutions the divergence from linear temperature profiles close to the rigid walls do not exceed 1% (0.1 K on $\Delta T = 10.0$ K) while concentration profiles have significant differences (compare solid and dashed lines in Fig. 7b). Thus small horizontal temperature gradients at the corners have strong impact on mass transfer in liquids. Note that small "spike" on the upper isotherm in Fig. 8 is just defect of phase unwrapping, actual isotherm should be smooth.

Despite our enormous efforts convection was remaining in the corners of the cell due to horizontal gradients. The origin of convection was analyzed in depth with support of 3D numerical simulations and will be published elsewhere. The results of that study showed that the major reason for the existence of horizontal temperature gradients is the poor heat transfer through rubber sealing near the junction lines: liquid, glass, and copper.

To identify the region of the convection spreading in bulk a dedicated set of experiments have been carried out. A few iso-dense tracer particles were placed in pure water and flow visualization experiments were aimed at particle tracing. The experimental results disclose the settings of convection and its impact on the concentration field. The trajectory of particles are superimposed on the distribution of stationary concentration field in Fig. 9a. The lines of equal concentration are shown at the end of the thermodiffusion experiment, $t \approx 140$ h. The particle velocities are given in Fig. 9b where the dashed line corresponds to the motion at the upper part and the solid line corresponds to the velocity of particle near the bottom. Note, that the velocities of the individual particles along trajectory are shown and not the velocity of the flow. So, the velocities perform fluctuations in time depending on the particle position. The velocity of the fluid motion, estimated by the $x - z$ projection of particles tracks, varies in the range of 10–35 μm/s. Mean values of particles speed are about 15 and 20 μm/s. Movement in the upper vortex is slightly faster in average. The non-equal size of vortices at upper and bottom parts is related to the temperature dis-

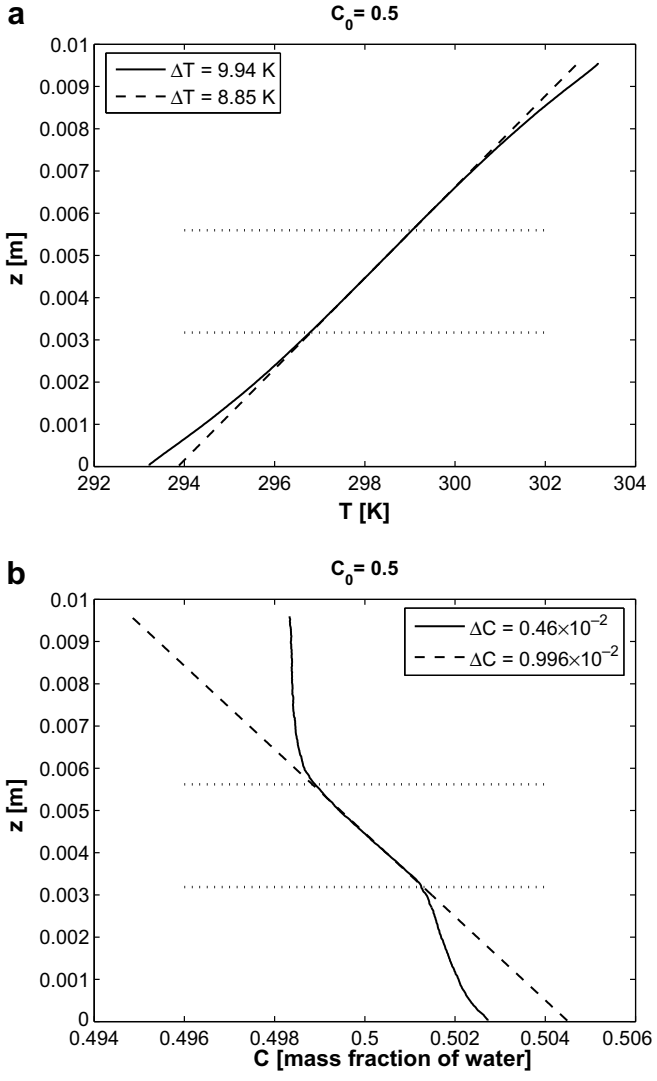

Fig. 7. Temperature (a) and concentration (b) profiles in steady state for water/isopropanol mixture with $C_0 = 0.5$; $t = 110$ h $\approx 5\tau_r \approx 4\tau_D$. Solid curves correspond to measured values and dashed lines show extension of the linear behavior in central part of the cell.

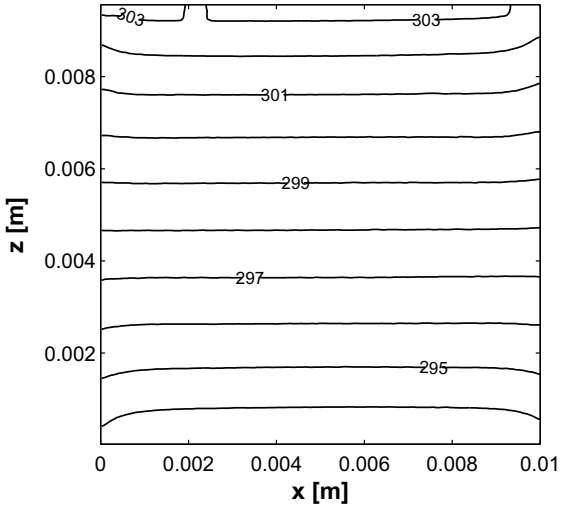

Fig. 8. Stationary temperature field for water/isopropanol mixture with $C_0 = 0.5$: isotherms are shown at the beginning of the experiment $t = 1200$ s; heating from above.

tribution in the ambient gas. These vortices would be equal in size if the temperature of the ambient gas would be symmetrical with respect to mid-plane $z = h/2$. These very weak motions in the corners, i.e. a few microns per second, mix up the solution introducing relatively strong perturbations of concentration profile. The strength of the convection slightly decreases with diminishing ΔT. One important conclusion can be drawn from these results is that the flow does not penetrate into the bulk, being concentrated in the corners. The distributions of the velocity fields give us reason to believe that the concentration profile measured at the central part of the cell is correct, not being modified by the localized motions.

All the methods, developed to measure the thermodiffusion coefficients, use temperature gradients in gravity field. Thus all of them have to face the problem of parasitic convection in the experimental cell, although it can be small or negligibly small. Horizontal temperature gradients may arise also in experiments in an elongated cavity (horizontal slot). Experiments in very thin gaps between cold and hot regions, i.e. a few microns, can also be affected by convection especially in the case of side heating. The time of the motion development for such systems is very short, $\tau_{vis} = L^2/v$. To the best of our knowledge we did not find in the literature experimental plots of $T(z)$ and $C(z)$ profiles related to this problem. Such profile can be obtained indirectly from the paper by Colombani et al. [22], where they show the evolution of concentration fringes during a thermal diffusion experiment from $t = 0$ to $t = 202$ h. The fringes in their Fig. 3 corresponding to $t = 202$ h are not equidistant in space, which indicates that $C(z)$ is not linear.

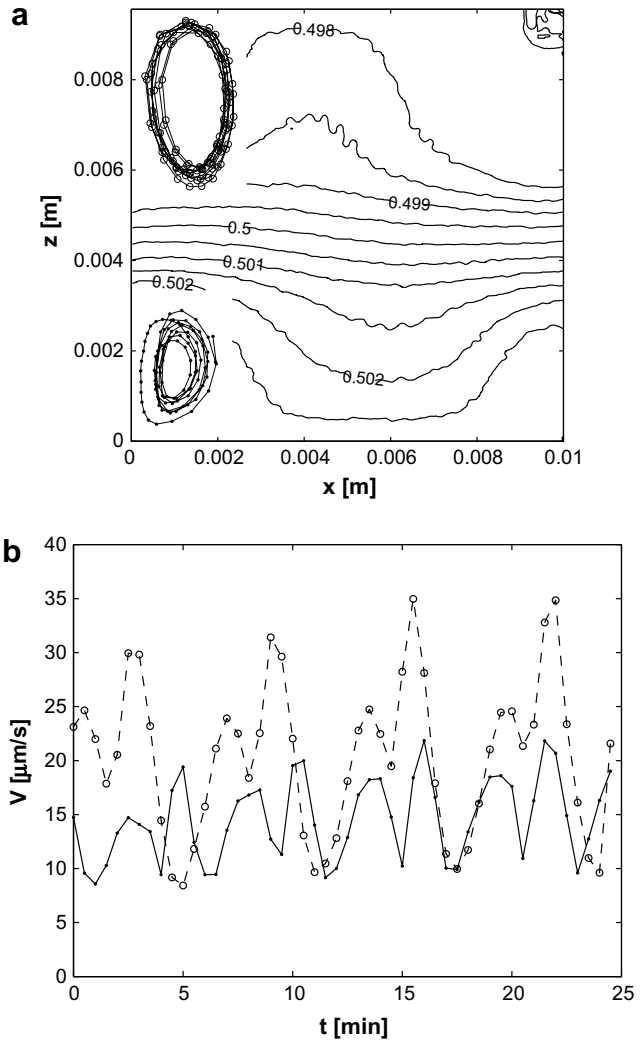

Fig. 9. Study of residual convection in the experimental cell. (a) Trajectory of tracer particles recorded each 30 s in water and isolines of concentration. (b) The velocity of particles along trajectory: solid and dashed curves correspond to particles located at lower and upper parts, respectively.

6.2. Convection free region

Analysis of temperature fields at numerous experiments proved that if convection exists, it appears as small vortices along the junctions. Results reported in Figs. 7 and 8 confirm these conclusions, where the linear behavior is well kept in the central part of the cell.

According to the different dynamics we can divide the whole cell in three zones, which are shown by dotted lines in Fig. 7. At the upper part, with the strongest convection in the corners, the solution is well mixed, and the concentration is almost independent of height. In the lower part, where the corner convection is weaker, the concentration profile varies with height due to thermodiffusion, but it is disturbed by the convection. The central zone between the dotted lines is free from convection. Thermodiffusion is responsible for the separation process in this area. In general the concentration field in the cell is described by

$$\frac{\partial C}{\partial t} = -\nabla \mathbf{j_C} \quad \text{where}$$
$$\vec{j}_C = \rho_0[\vec{V}C - D\nabla C - D_T C_0(1 - C_0)\Delta T/L] \tag{14}$$

Let us cropping out the area between the dotted horizontal lines in Fig. 7b where the concentration profile is linear. In this area the velocity is equal to zero and the mass flux is also equal to zero at steady state. So in this cropped area the Soret coefficient is determined from Eq. (14) as

$$S_T = \frac{D_T}{D} = \frac{1}{C_0(1 - C_0)}\frac{(\Delta C)}{(\Delta T)} = \frac{1}{C_0(1 - C_0)}\frac{(\partial_z C)}{(\partial_z T)} \tag{15}$$

By doing this we can determine the component separation ΔC corresponding to the ideal thermodiffusion conditions (without convection). The linear profiles of T and C in this cropped area are extended over the entire cell with the same slopes as shown by the dashed lines in Fig. 7. We can use in Eq. (15) the values of ΔT and ΔC at the level of dotted lines or their extension, the results will of course be the same.

The following approach is used for measurements of diffusion and Soret coefficients. Over the entire duration of the experiment the data are recorded and the figures, similar to Fig. 7 are obtained for all available interferograms

in time. Computerized analysis of concentration profiles, similar to Fig. 7b, identifies the boundary of the convection-free area during complete experiment. The steady state at this area corresponds to zero mass flux and Eq. (13) is valid. Moreover, knowing the boundary of motionless region we may processed recorded data according Eq. (13) where at each time step ΔT and ΔC are calculated for the region between dotted lines shown in Fig. 7. In this way we may determine both the Soret and diffusion coefficients. Strictly speaking the condition of zero mass flux, leading to Eq. (11) in the theoretical approach, is not fulfilled out of steady state. Keeping in mind that this approach is often used in practice we adopted it to our experiments. At the following section we will show that the convection-free zone is identified correctly and the assumptions of the theoretical model are fulfilled sufficiently well at the boundaries of this zone.

6.3. Validation of suggested experimental method: water/ethanol mixture

Taking into account all problems and their solutions described above a dedicated set of experiments has been performed for the justification of the suggested method. Among the aqueous systems there is a considerable amount of data for measurements of the Soret coefficient in water/ethanol mixture and this mixture was chosen for the validation of the technique. The largest amount of literature data are accumulated for two different compositions: with mass fraction of water ≈0.5 and ≈0.6. Our experiments were carried out for the mixtures with close compositions: 0.491, 0.602, and 0.613. This choice is due to degassing procedure, which was employed to prevent appearance of bubbles in the experimental cell. Because of different values of saturation vapor pressure for water and alcohol, the composition of mixture changes during degassing procedure approximately by 2%. The composition of final mixture was checked by a refractometer.

The time evolution of the concentration separation $\Delta C(t)$ for the mixture with initial content of water $C_0 = 0.602$ is shown in Fig. 10a. The mean temperature of the system is $T_{\text{mean}} = 295.5$ K and the applied $\Delta T = 9.87$ K. The data along the curve were collected over the central (non-disturbed) part of the cell. The fitting curve was obtained on the basis of the approach, described in Section 5, and applied for the central part only.

The diffusion coefficients, using the present method, along with results from other techniques are shown in Fig. 10b. Let us note the variety of methods used by different authors: diaphragm cell technique by Hammond and Stokes [23], Taylor dispersion technique by Pratt and Wakeham [25] and Harris et al. [24], open-ended capillary by Dutrieux et al. [27], thermal diffusion forced Rayleigh scattering (TDFRS) method by Kita et al. [26], and digital interferometry (present method). The working temperature at three first references was 298 K, whereas the three other authors worked at 295.5 K. The points obtained by Taylor

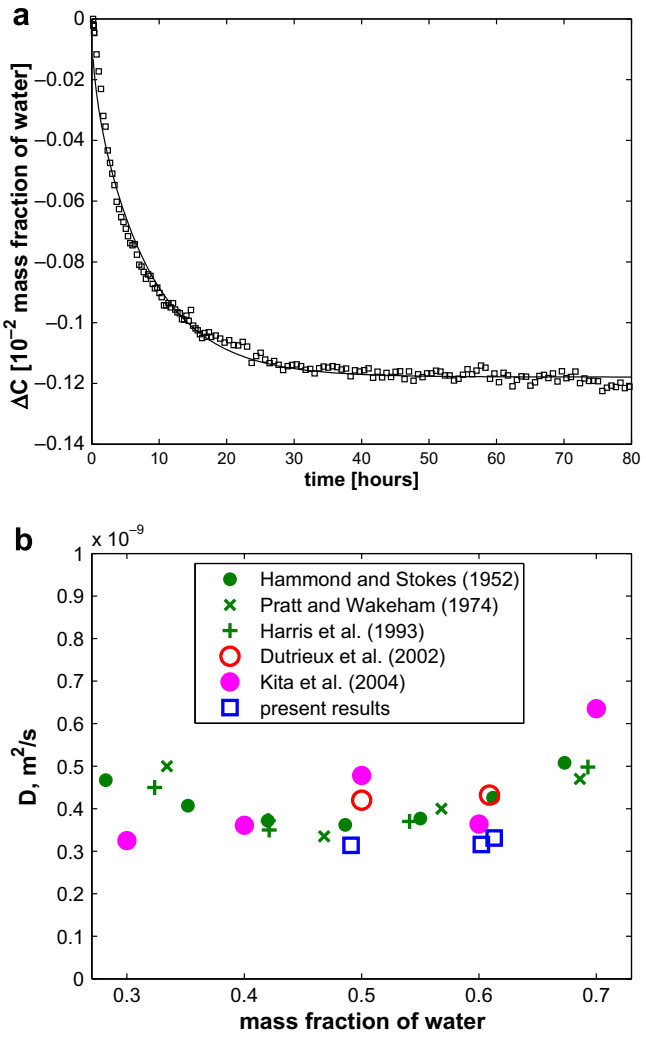

Fig. 10. (a) Time evolution of concentration separation $\Delta C(t)$ for water/ethanol mixture for $C_0 = 0.61$. (b) Diffusion coefficient of water/ethanol as a function of mass fraction of water in present work (open cube) and from Hammond and Stokes [23], Pratt and Wakeham [25], Harris et al. [24], Dutrieux et al. [27], and Kita et al. [26]. Symbols are indicated on the plot.

dispersion method and by the diaphragm cell technique are close to each other. Moreover, their values would not be disturbed by buoyancy induced convection as they are performed in isothermal conditions. The results by Dutrieux et al. [27] (open capillary), Kita et al. [26] (TDFRS), and the present results are scattered around the above mentioned data. The diffusion coefficient, even if it is temperature dependent, should not change too much over a 2.5 K temperature range. A possible explanation of the larger scattering follows from the fact that the last two authors (Kita and current authors) use indirect methods of determining the diffusion coefficient, namely some fitting procedure from thermodiffusion data. Note, that our values are located at the bottom part of the experimental cloud of points. If convection would be present in the central area of the plot it would increase the value of the diffusion coefficient. As a conclusion, our results are in the general trend

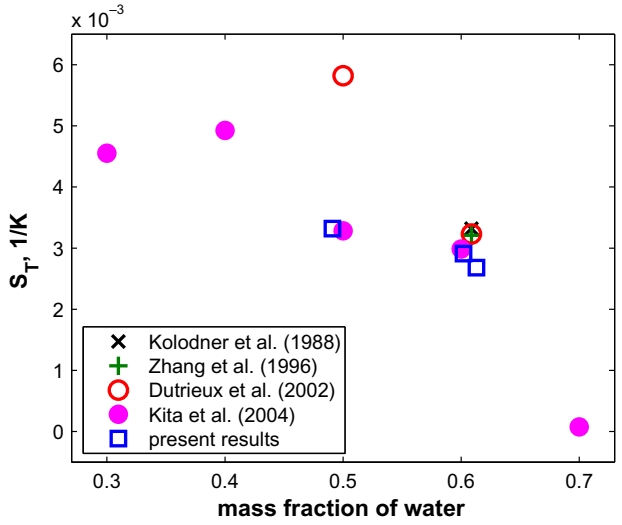

Fig. 11. Soret coefficient of water/ethanol as a function of mass fraction of water in present work (open cube) and from Kolodner et al. [10], Zhang et al. [11], Kita et al. [26], and Dutrieux et al. [27].

of other ones, and prove that the suggested technique is competitive. The measured values provide a solid argument that the convection-free zone is identified correctly and that the condition of zero mass flux holds satisfactorily well at the boundaries of this zone.

The Soret coefficients for water/ethanol mixture were calculated on the basis of fitting curve, Eq. (13), and using the steady state, Eq. (15). The obtained values slightly differ: e.g. for $C_0 = 0.613$ they are $S_T = 2.82 \times 10^{-3}\,\mathrm{K}^{-1}$ and $S_T = 2.88 \times 10^{-3}$ 1/K, respectively.

The measured and literature data for Soret coefficients are summarized in Fig. 11. The techniques used by different authors are: beam deflection by Kolodner et al. [10] and Zhang et al.[11], optical TDFRS method by Kita et al. [26], mean results from TGC (thermogravitational column) and LDV (laser Doppler velocimetry) by Dutrieux et al. [27], and digital interferometry (present method). Although they are obtained at different temperatures, they should not change too much over a 2.5 K temperature range. The background results taken from Fig. 4 in [26] are shown by filled circles. The major part of results are focused around $C_0 = 0.609$. The results of different authors shown in Fig. 11 are listed in Table 1 for compositions close to $C_0 = 0.5$ and $C_0 = 0.609$ in the order of the temperature rise. The mean value of Soret coefficient for $C_0 = 0.609$ is $S_T = 3.18 \times 10^{-3}\,\mathrm{K}^{-1}$ and could be considered as a benchmark value. Linear interpolation of our results from measurements at $C_0 = 0.491$ and $C_0 = 0.602$ gives $S_T = 3.00 \times 10^{-3}\,\mathrm{K}^{-1}$ at $C_0 = 0.609$, which has only 5% deviation from the "benchmark" value. It falls into the range of average deviations by other authors. The point $C_0 = 0.491$ was chosen for the calculation of S_T value at the benchmark point $C_0 = 0.609$, as our experiments around the point $C_0 = 0.49 \pm 2\%$ were repeated the most. There are only two results at $C_0 \approx 0.5$ by Kita et al. [26] and Dutrieux et al. [27] and they are very different. To be confident in our final value for this composition the experiments were repeated at different ΔT. Our results are closest to those by Kita et al. [26], which were obtained by another optical method, (TDFRS). To conclude this validation section: the method of digital interferometry appears to be reliable and it determines diffusion and Soret coefficients consistent with those available in the literature.

6.4. Measurements diffusion and Soret coefficients in water/isopropanol mixture

The recently measured Soret coefficients for water/isopropanol mixture provoke a lot of discussions during the Congresses, although the only published data by Poty et al. [28] are relatively old (1974) and some points in their measurements look suspicious. It explains our choice of this system under investigation.

In the beginning the results obtained on the basis of time-dependent behavior of the system will be discussed. Time evolution of concentration differences between top and bottom within the cell, $\Delta C(t)$, similar to Fig. 4 was made for all studied mixtures. Although the data used for reporting in Fig. 4 were gathered prior to comprehensive study of the environmental conditions around the cell and the daily variations of the temperature were detected. Experimental results in this section were obtained at best experimental conditions and the processing was done using the information only from the central part of the cell. Thus the same procedure as in previous Section (measurements in convection-free zone) was used for the measurement of diffusion and Soret coefficients in water/isopropanol mixture.

The only results by Pratt and Wakeham [29] for diffusion coefficients (dated back to 1975) were found in literature for this mixture. These results along with present ones are summarized in Fig. 12. The data was obtained by completely

Table 1
Soret coefficients for water/ethanol mixture

	Kita et al. [26] $T = 20$ °C	Dutrieux et al. [27] $T = 22.5$ °C	Present result $T = 22.5$ °C	Kolodner et al. [10] mean value $T = 20$ °C and 25 °C	Zhang et al. [11] $T = 25$ °C
$C_0 = 0.491$			3.32 ± 0.016		
$C_0 = 0.5$	3.28	5.82			
$C_0 = 0.602$			3.01 ± 0.015		
$C_0 = 0.609$	2.98	3.23	3.0 interpolation	3.32	3.21
$C_0 = 0.613$			2.88 ± 0.013		

Experimental data.

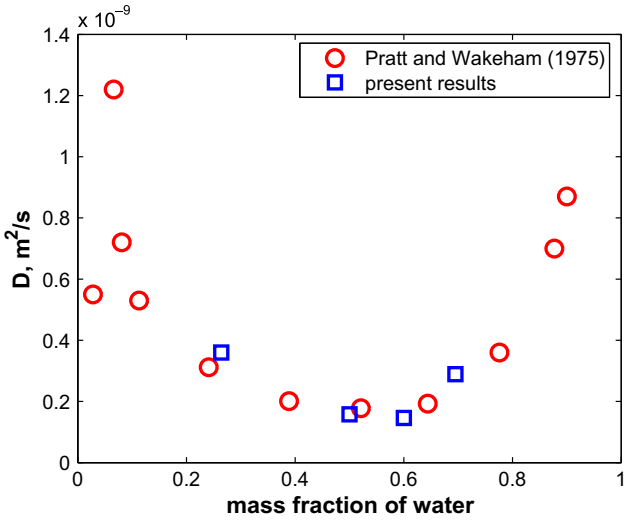

Fig. 12. Diffusion coefficient of water/isopropanol as a function of mass fraction of water in present work (open cube) and from Pratt and Wakeham [29] (open circles).

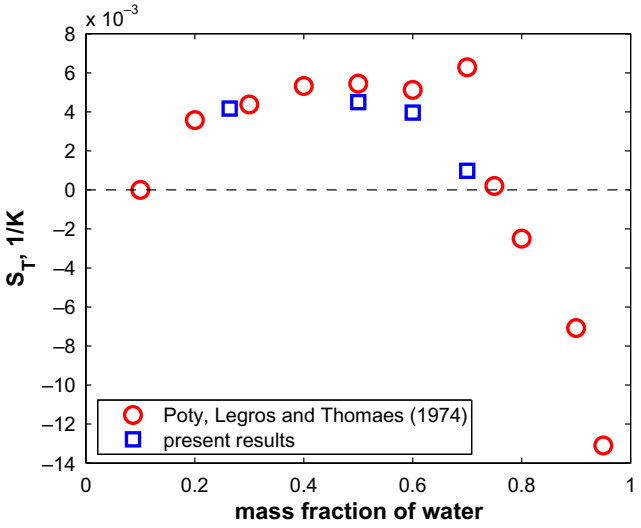

Fig. 13. Soret coefficient of water/isopropanol mixture as a function of mass fraction of water in present work (open cube) and by Poty et al. [28] by open circle.

different methods: Taylor dispersion technique at isothermal conditions was used by Pratt and digital interferometry in non-isothermal environment is utilized in present method. The working temperature used by Pratt was $T = 298$ K, while in our case it is the mean temperature, i.e. $T_{mean} = 298$ K. Independent measurements yield excellent agreement in the determination of the diffusion coefficient. This agreement once more confirms that the condition of zero mass flux at non-steady conditions are properly satisfied on the boundary of the convection-free zone.

The Soret coefficients in water/isopropanol system were measured for the same compositions as diffusion. Our experimental points, shown in Fig. 13, are obtained for the applied temperature difference $\Delta T \approx 10$ K. Comparison of present results with the previous results by Poty et al. [28] in Fig. 13 demonstrates from very good to moderate agreement between sources. At the mixture with low concentration of water the agreement is excellent. Divergence between results slightly grows with increasing of water content. Obviously the results from [28] are not exact in the vicinity of point $C_0 = 0.7$ (before sign change). This point looks like "wild point". According to the general trend of $S_T(C)$ in Fig. 13 our results appear most trustworthy.

Quantitative comparison of the results for different initial compositions and various experimental conditions are given in Table 2. Soret coefficients corresponds to the values obtained on the basis of information from the central part of the cell in steady state. Table 2 includes not only results for different compositions (shown also in Fig. 13) but also demonstrates result for different experimental conditions for the system with mass fraction of water $C_0 = 0.5$. The column, which is one before last, shows results for $C_0 = 0.5$ for applied temperature difference $\Delta T \approx 5$ K where one would expect the weaker convection in the system. The difference between the Soret coefficients, measured at $\Delta T \approx 10$ K and $\Delta T \approx 5$ K is less than 3%. It emphasizes that both measurements are coming from well determined convection-free zone, although the size of these zones can be different.

Last column reveals results of the experiment, when air around the diffusion cell was not thermostabilized, corresponding time dependence is shown in Fig. 4. The value of S_T obtained under these experimental conditions is much lower than the values, measured at conditions of controlled temperature around the cell.

7. Conclusions

We have presented a novel experimental technique based on optical digital interferometry for investigating the thermodiffusion process in liquids and measuring mass transport coefficients. Digital interferograms are recorded at a selected rate during the observation of heat and mass

Table 2
Experimental data for Soret coefficients in water/isopropanol mixture, $T_{mean} = 298$ K

C_0	0.264	0.5	0.6	0.7	0.5	0.5
Experimental condition					Different ΔT	Open air
Applied ΔT (K)	9.89	9.94	10.2	10.38	4.94	10.19
10^{-3} S_T (1/K)	4.17	4.51	3.96	0.98	4.39	3.29

Error bars for given S_T is about 5%.

transport in the liquid. Knowledge of the spatial distribution of the total phase shift gives information about changes in the refractive index. In turn, it defines the local gradients of composition inside the fluid both for steady state and dynamic regimes. Different steps of image processing and obtaining results were discussed in details.

All methods developed to measure thermodiffusion coefficients are affected by convection to one extent or another. Unlike previously developed methods the present one allows to "see" and analyze the situation inside the cell. The experiments were carried out in a relatively large cubic cell, $L = 0.01$ m. The large view over the entire cell allowed us to identify the settings of convection. It was ascertained that convective flows do not penetrate into the bulk. This enabled measurements of the transport coefficients according to the information about $T(z)$ and $C(z)$ in the central part of the cell, the so called the convection-free zone.

Moreover, it appears that on the boundaries of the convection-free zone the condition of zero mass flux is well satisfied during the whole diffusion process and not only in steady state. This condition is important to the companion theoretical approach and its fulfillment was proven by the measurements of the diffusion coefficients. The Soret coefficient can be determined from the steady state condition while the diffusion coefficients can only be obtained from records within the time dependent process. The excellent agreement of the measured diffusion coefficients with those available in the literature for water/ethanol and water/isopropanol mixtures is strong evidence that the convection-free zone is identified correctly.

The method has undergone an extensive scientific validation against recent published data for water/ethanol mixtures. The quantitative comparison of diffusion and Soret coefficients reveals excellent agreement with published data. This method was applied to the measurements of the Soret coefficients in water/isopropanol mixture. The obtained dependence of S_T on composition in water/isopropanol mixtures demonstrates the same tendency as previously obtained results (Ref. [28]).

Our experimental method was initially developed for future experiments in microgravity where buoyant convection is negligibly small. However, here we showed that it can be used in laboratory conditions even there are some zone affected by convection.

To conclude: the method of digital interferometry appears to be reliable and it determines diffusion and Soret coefficients consistent with those available in the literature.

Acknowledgements

We are indebted to Prof. J.C. Legros for helpful discussions and creating the academic environment that made this research possible. We are grateful to Dr. F. Dubois for valuable help in designing the optics. The authors wish to thank Dr. S. Van Vaerenbergh and Dr. I. Ryzhkov for helpful discussions.

References

[1] F. Montel, J. Bickert, J. Hy-Billiot, M. Royer, Pressure and Compositional Gradients in Reservoirs, SPE 85668-MS (2003).
[2] J.P. Severinghaus, T. Sowers, E.J. Brook, R. Alley, M. Bender, Timing of abrupt climate change at the end of the Younger Dryas from thermally fractionated gases in polar ice, Nature 391 (1998) 141.
[3] A. Firoozabadi, K. Ghorayeb, K. Shukla, Theoretical model of thermal diffusion factors in multicomponent mixtures, AIChE J. 46 (2000) 892–900.
[4] K. Haugen, A. Firoozabadi, On the unsteady state species separation of a binary liquid mixture in a rectangular thermogravitational column, J. Chem. Phys. 124 (2006) 1–10.
[5] B. Rousseau, C. Nieto-Draghi, J. Bonet Avalos, The role of molecular interactions in the change of sign of the Soret coefficient, Europhys. Lett. 67 (2004) 976–982.
[6] S. Pan, M.Z. Saghir, M. Kawaji, Ch.G. Jiang, Yu Yan, Theoretical approach to evaluate thermodiffusion in aqueous alkanol solution, J. Chem. Phys. 126 (2007) 01452.
[7] S. Wiegand, Thermal diffusion in liquid mixtures and polymer solutions, J. Phys.: Condensed. Matter 16 (2004) R357–R379.
[8] J.K. Platten, The Soret effect: a review of recent experimental results, ASME J. Appl. Mech. 73 (2006) 5–15.
[9] M. Giglio, A. Vendramini, Buoyancy-driven instability in a dilute solution of macromolecules, Phys. Rev. Lett. 39 (1977) 10141017.
[10] P. Kolodner, H. Williams, C. Moe, Optical measurement of the Soret coefficient of ethanol/water solutions, J. Chem. Phys. 88 (1988) 6512–6524.
[11] K.J. Zhang, M.E. Briggs, R.W. Gammon, J.V. Sengers, Optical measurement of the Soret effect and the diffusion coefficient of liquid mixture, J. Chem. Phys. 104 (1996) 6881–6892.
[12] S. Wiegand, W. Kohler, Measurements of transport coefficients by an optical grating technique, in: W. Kohler, S. Wiegand (Eds.), Thermal Nonequilibrium Phenomena in Fluid Mixtures, vol. LNP 584, Springer, 2002, pp. 189–210.
[13] B.-J. de Gans, R. Kita, S. Wiegand, J. Luettmer-Starthmann, Unusual thermal diffusion in polymer solutions, Phys. Rev. Lett. 91 (2003) 245501.
[14] A. Becker, W. Köhler, B. Müller, A scanning Michelson Interferometer for the measurements of the concentration and temperature derivative of the refractive index of liquids, Ber. Bunsen. Phys. Chem. 99 (1995) 600–608.
[15] J. Sengers, J.M. Ortiz de Zarate, Nonequilibrium concentration fluctuations in binary liquid systems induced by Soret effect, in: W. Kohler, S. Wiegand (Eds.), Thermal Non-equilibrium Phenomena in Fluid Mixtures, vol. LNP 584, Springer, 2002, pp. 121–145.
[16] J.K. Platten, J.C. Legros, Convection in Liquids, Springer, Berlin, 1984.
[17] W. Köhler, P. Rossmanith, Aspects of thermal diffusion forced Rayleigh Scattering: heterodyne detection, active phase tracking, and experimental constraints, J. Phys. Chem. 99 (1995) 5847–6838.
[18] Robert C. Reid, T.K. Sherwood, The Properties of Gases and Liquids: Their Estimation and Correlation, second ed., McGraw-Hill, New York, 1966.
[19] D.R. Lide (Ed.), CRC Handbook of Chemistry and Physics, 74th ed., CRC, London, 1993.
[20] W.B. Li, P.N. Serge, R.W. Gammon, J.V. Sengers, Determination of the temperature and concentration dependence on refractive index in liquids, J. Chem. Phys. 101 (1994) 5058.
[21] A. Mialdun, D. Melnikov, V. Shevtsova, Observation of diffusion phenomena in ground experiments: problems and solutions, IAC-06-A2.4 (57th IAC Meeting, Valencia, Spain, October 2006), p. 12.
[22] P. Colombani, H. Dez, J. Bert, J. Dupuy-Philon, Hydrodynamic instabilities and Soret effect in aqueous electrolyte, Phys. Rev. E 58 (1998) 3202–3208.
[23] B.R. Hammond, R.H. Stokes, Diffusion in binary liquid mixtures. Part 1. Diffusion coefficients in the system ethanol + water at 25, Trans. Faraday Soc. 49 (1953) 890–895.

[24] K.R. Harris, T. Goscinska, H.N. Lam, Mutual diffusion coefficients for the systems water–ethanol and water–propan-1-ol at 25 °C, J. Chem. Soc., Faraday Trans. 89 (1993) 1969–1974.
[25] K.C. Pratt, W.A. Wakeham, The mutual diffusion coefficients of ethanol-water mixtures: determination by rapid, new method, Proc. R. Soc. Lond. Ser. A – Math. Phys. Sci. 336 (1974) 393–406.
[26] R. Kita, S. Wiegand, J. Luettmer-Strathmann, Sign change of the Soret coefficient of poly(ethylene oxide) in water/ethanol mixtures observed by thermal diffusion forced Rayleigh scattering, J. Chem. Phys 121 (2004) 3874–3885.
[27] J.F. Dutrieux, J.K. Platten, G. Chavepeyer, M.M. Bou-Ali, On the measurements of positive Soret coefficients, J. Chem. Phys. 106 (2002) 6104–6114.
[28] P. Poty, J.C. Legros, G. Thomaes, Thermal diffusion in some binary liquid mixtures by the flowing cell methods, Z. Naturforsch. 29A (1974) 1915–1916.
[29] K.C. Pratt, W.A. Wakeham, The mutual diffusion coefficient for binary mixtures of water and the isomers of propanol, Proc. R. Soc. Lond. Ser. A – Math. Phys. Sci. 342 (1975) 401–419.